Simulation of Exergy Analysis & Heat Transfer of Shell and Multi Pass Heat Exchanger

Shishir Seluker[1]; Dr. Mohammed Ali[2], Dr. Chetan Jaiswal[3]

Abstract

The heat exchanger (HX) is a critical component in several sectors, since it effectively enhances heat transfer rates, hence reducing energy consumption. This work examines the numerical modeling of a shell and double tube heat exchanger, both with and without baffles, in order to assess the heat transfer with exergy analysis. A computational fluid dynamics (CFD) program called ANSYS (Fluent) is used to do a numerical simulation of a 3D model with turbulent flow between the range of 4000 to 12000. The circular vent baffles concept is employed on the lateral surface of the shell. The simulation findings indicate that the circular vents located on the baffles of the heat exchanger having a notable influence on both the thermal-hydraulic performance and the exergy analysis. Furthermore, the findings indicate that the heat exchanger's efficacy is enhanced by 21% when baffles are incorporated, particularly at high Reynolds numbers, in comparison to a heat exchanger with no baffles. In addition, the exergy loss reached its maximum value of 48W when baffles were present. In conclusion, it has been determined that the heat exchanger equipped with baffles exhibits superior hydraulic and thermal efficiency compared to the heat exchanger with no baffles.

[1]Research Scholar, Department of Mechanical Engineering, Oriental University, Indore (M.P.), India
shishirseluker@gmail.com
[2]Professor, Department of Mechanical Engineering; Oriental University, Indore (M.P.), India
hasnaat_2005@yahoo.co.in
[3]Associate Professor, Mechanical Engineering Department, Oriental University Indore (M.P.), India
chetan.jaiswal2083@gmail.com

Keywords: double tube heat exchanger, CFD, exergy analysis, baffles, turbulent flow

Introduction

The topic of energy conservation is highly significant in the current century and is expected to be a major concern in the next years. Technological advancements in cooling and heating procedures for industrial appliances result in energy conservation, enhanced heat transmission, and prolonged device lifespan. Various types of heat exchangers (HXs) are employed in many industrial sectors such as the petrochemical industry, chemical and nuclear reactors, power plants for condensation and boiling, and air-conditioning and refrigeration processes [1]. A "heat exchanger" may be defined as a device that efficiently transfers energy between two fluids, maximizing the rate of transfer while minimizing operational expenses [1]. Based on the design, the majority of heat exchangers (HXs) incorporate the tubular form, which is extensively employed in many industries [2]. In this heat exchanger, a single fluid circulates through the tubes while another fluid flows through the shell around the bundle of tubes [3]. The classification of tubular heat exchangers includes shell and tube heat exchanger (STHX), double tube heat exchanger, and coiled tube heat exchanger [4]. The twin tube heat exchanger has exceptional heat transfer efficiency, particularly when equipped with a straight baffle configuration. Baffles are often positioned on the fluid side of the shell to enhance the convection coefficient by promoting turbulence. Additionally, these structures provide physical support for the tubes. Figure 1 [5] depicts a twin tube heat exchanger with baffles, consisting of two shells.

Several study investigations have been carried out on the circular double tube heat exchanger in recent years. Pamuk [6] utilized numerical modeling to investigate the impact of baffles on concentric tube heat exchangers. He evaluated two distinct models: one is a basic HX model with baffles, while the other is an enhanced variant with three baffles. The numerical findings demonstrated that ANSYS Fluent provides precise outputs about heat transfer and hydrodynamics in fluid flow during the process Concentric tube heat exchanger. The velocity, pressure, and temperature distribution within the oil flow inside the HX were also demonstrated. Etghani and Baboli [7] conducted a numerical study and optimization to assess the thermal conditions and exergy loss of a shell with a helical tube heat exchanger. Their work suggested a model with laminar flow in three dimensions. An examination was conducted on the impacts of four parameters: tube diameter, pitch coil, cold flow rate, and hot flow rate. The researchers concluded that the cold flow rate and tube width were the primary factors affecting exergy loss and heat transfer. In their study, Fahad et al. [8] utilized numerical modeling to accurately ascertain the thermal characteristics of a STHX (Shell and Tube Heat Exchanger) equipped with baffles, operating under laminar flow conditions. The researchers investigated the impact of several angles of tube baffles (-45°, 0°, and 45°) on the efficiency of the heat exchanger. Based on their investigation, they noted that the use of baffles set at a 45° angle enhances the rate of heat transfer at high Reynolds numbers. Zhou et al. [9] conducted a numerical analysis to examine the heat transfer and pressure drop properties of forced convection in the STHX with trefoil-hole baffles. Their findings demonstrated that the fluid flow reached a fully evolved state after passing through the first hole's baffle. Additionally, it was discovered that the heat transfer coefficient and pressure drop exhibited periodic variations throughout the axial length. Teja and Narasimha Rao [10] created a three-dimensional numerical model for a heat exchanger (HX) that includes hexagonal vent baffles. The researchers investigated the enhancement of heat transfer by computational fluid dynamics (CFD) simulation in the presence of turbulent flow. The results indicated that the coefficient of heat transmission was consistently greater for hexagonal vent baffles, independent of the placement of the hexagonal vents on different tubes. Santhisree et al. [11] provided an analysis of the thermal and hydraulic efficiency of a heat exchanger with 4 baffles and 22 tubes. The temperature analysis was simulated using CFD software. In addition, the velocity, temperature, and pressure counters were implemented. In their study, Sadikin et al. [12] examined the impact of the number of baffles and the space between them.

Their numerical study was conducted using computational fluid dynamics (CFD) simulation for a three-dimensional (3D) model. The findings indicated that both the quantity and arrangement of baffles in the heat

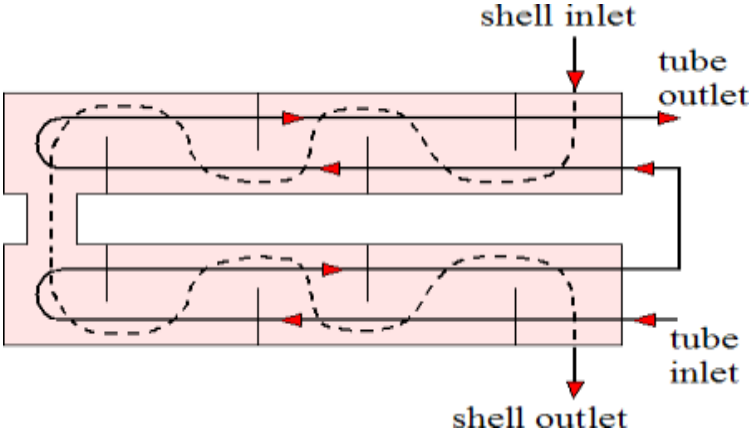

exchanger (HX) have a significant impact on the pressure drop and flow pattern. The authors dos Santos Filho et al. [13] presented a mathematical model for STHX.

Figure 1. Two shell passes and double tube heat exchanger with baffles [5]

The baffles affect the pressure drop and flow in the STHX. Their numerical study was conducted using computational fluid dynamics (CFD) simulation for a three-dimensional (3D) model. They observed through simulation that the effectiveness of thermal exchange increased with presence of baffles. Also, they presented the counters of fluid behaviors. Yang and Liu [14] introduced numerical and experimental report to reveal the properties of flow and heat transfer of STHX. They used in their numerical simulation of HX with plate and rod baffles. The results measured of their experiments and simulation analysis showed that, the Nusselt number for the HX with plate baffles was around 128-139% of that for the HX with rod baffles. Kirinčić et al. [15] presented a numerical and experimental study of a small size STHX with segmental baffles. They considered a 3D model with laminar flow and steady state. Hence, they found a very well agreement between experimental investigation and the numerical modelling of the heat transfer problem.

The objective of this study is to replicate the thermal characteristics and conduct an exergy analysis of a three-dimensional model in a shell and double tube heat exchanger, both with and without baffles. This type comprises a single pass of the shell, equipped with circular vents and baffles, and four passes of tubes. The objective is to enhance the surface area available for heat transfer. The numerical computation involves solving the governing equations using the steady state, incompressible, and (k-ε) model.

Mathematical Modelling

Geometrical model descriptions

Table 1. Dimensions of heat exchanger

Description	**Size**
Shell diameter	24 mm
Inlet and outlet diameter of shell	3 mm
Tube internal dimeter	2 mm
Tube external dimeter	2.2 mm
Tube thickness, δ_t	0.1 mm
Total tube length	200 mm
Heat exchanger length, L	52 mm
Number of baffles	2
Baffle spacing	26 mm
Baffles thickness	0.3 mm
Diameter of vent circle	3 mm
Baffle inclination	0°

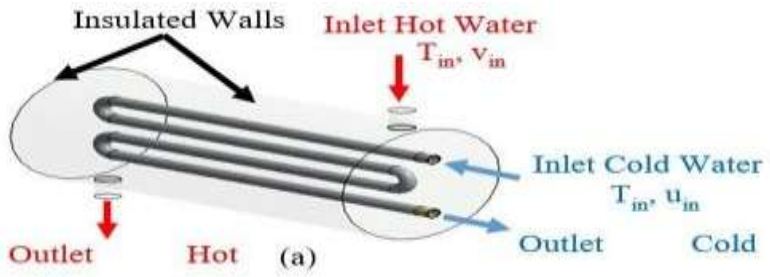

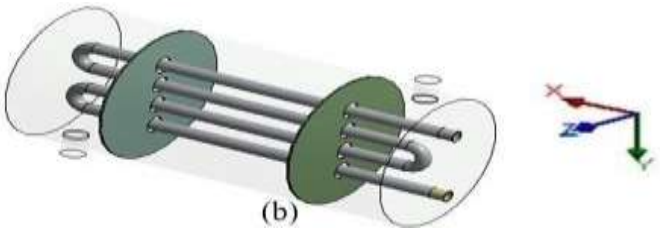

Figure 2. Three-dimensional diagram for heat exchanger: (a)without baffles, (b) with baffles

The geometry (3D) of the numerical simulation is presentedin Figure 2 which represents the shell and double tube HX without and with baffles respectively. It consists of one pass atthe shell and four passes of tube. The dimensions details of theheat exchanger are listed in Table 1. Generally, cold water flows through the double tube and is heated by a cross-parallelflow of hot water passing in the shell. Two baffles with circularvents are used at a fixed angle around the shell diameter to promote heat transfer. To simplify computation domain, several basic assumptions are made:

- Heat transfer and fluid flow were in three-dimensional andsteady state.
- The fluid flow for tube and shell sides was turbulent andincompressible.
- The thermo and physical properties of fluids were independent of temperature.
- Gravity effect was negligible.
- Baffles and tube wall separating between hot and cold fluids were considered Aluminium walls.

Governing Equations

Depending on the above assumptions, the governing equations for turbulent flow (k-ε) model and steady state heat transfer problem can be presented below in cartesian coordinate system [16]:

(I). Continuity Equation

$$\frac{\partial u_j}{\partial x_j} = 0$$

(II). Momentum Equation

$$\frac{\partial(u_i u_j)}{\partial x_j} = -\frac{1}{\rho}\cdot\frac{\partial P}{\partial x_i} + \frac{1}{\rho}\cdot\frac{\partial}{\partial x_j}\left[\mu_{eff}\left(\frac{\partial u_i}{\partial x_j} - \frac{\partial u_j}{\partial x_i}\right)\right]$$

(III). Energy Equation

$$\frac{\partial(C_P u_j T)}{\partial x_j} = \frac{1}{\rho}\cdot\frac{\partial}{\partial x_j}\left(\lambda_{eff}\frac{\partial T}{\partial x_j}\right)$$

where, P, T and u refer to fluid pressure, temperature and velocity respectively; Cp and ρ stand for specific heat Constant pressure and density of fluid respectively; μ_{eff} is the effective dynamic viscosity and can be calculated by the sum the dynamic viscosity of laminar and turbulent:

$$\mu_{eff} = \mu_l + \mu_t$$

The effective thermal conductivity, λ_{eff} equal to:

$$\lambda_{eff} = \lambda_l + \lambda_t C_P / Pr_t$$

where, Pr_t refer to turbulent Prandtl number, λ_l and λ_t are the laminar and turbulent conductivity.

The model of standard k-ε turbulence is considered with standard wall function for the present computation. The transport equations of kinetic energy of the turbulence and its dissipation rate are as follow:

The turbulence kinetic energy k:

$$\frac{\partial(k u_j)}{\partial x_j} = \frac{1}{\rho}\cdot\frac{\partial}{\partial x_j}\left[\left(\mu_l + \frac{\mu_t}{\sigma_k}\right)\frac{\partial k}{\partial x_j}\right] + \frac{G_k}{\rho}\varepsilon$$

The rate of dissipation of the turbulence kinetic energy ε:

$$\frac{\partial(\varepsilon u_j)}{\partial x_j} = \frac{1}{\rho}\cdot\frac{\partial}{\partial x_j}\left[\left(\mu_l + \frac{\mu_t}{\sigma_\varepsilon}\right)\frac{\partial \varepsilon}{\partial x_j}\right] + \frac{C_{1\varepsilon}\varepsilon}{\rho k}G_k - C_{2\varepsilon}\frac{\varepsilon^2}{k}$$

where,

$$\mu_t = \rho C_\mu \frac{k^2}{\varepsilon};\ G_k = 2\mu_t E_{ij}\cdot E_{ij};\ E_{ij} = \frac{1}{2}\left(\frac{\partial u_i}{\partial x_i} + \frac{\partial u_i}{\partial x_j}\right)$$

The constant for the current turbulent model is set as below:

$$C_\mu = 0.09; C_{1\varepsilon} = 1.44; C_{2\varepsilon} = 1.92;\ \sigma_k = 1.0; \sigma_\varepsilon = 1.3$$

Boundary Conditions

The boundary conditions for modelling are shown in Figure 2. Generally, there are two inlets and two outlets in shell and double tube HX. The inlets are defined as velocity with temperature and outlets are defined as pressure outlets. Different Reynolds numbers ranging from 4000 to 12000 are used for cold and hot water at inlet region. Inlet temperature of tube and shell are adopted at 300 K and 360K respectively. The shell walls are considered as insulated. The baffles and tube wall separating between hot and cold fluids are considered as domain interface wall. The boundary conditions for the numerical calculation are set below:

Various inlet conditions for the problem are-

u= u_{in}, $v = w = 0$, $T = T_{in}$ for tube side

v = v_{in}, $u = w = 0$, $T = T_{in}$ for shell side

Various outlet conditions for the problem are as follows-

$$\left.\begin{aligned} &\frac{\partial u}{\partial x} = \frac{\partial v}{\partial x} = \frac{\partial w}{\partial x} = 0, \frac{\partial T}{\partial x} \\ &\frac{\partial k}{\partial x} = \frac{\partial \varepsilon}{\partial x} \text{ and } P_{out} = 0 \end{aligned}\right\} \text{for tube side}$$

$$\left.\begin{aligned} &\frac{\partial u}{\partial y} = \frac{\partial v}{\partial y} = \frac{\partial w}{\partial y} = 0, \frac{\partial T}{\partial y} \\ &\frac{\partial k}{\partial y} = \frac{\partial \varepsilon}{\partial y} \text{ and } P_{out} = 0 \end{aligned}\right\} \text{for shell side}$$

Walls are of two types in the current problem- external & internal walls. Boundary conditions for external walls are as follows-

$u = v = w = 0$ & $\frac{\partial T}{\partial x} = \frac{\partial T}{\partial y} = \frac{\partial T}{\partial z} = 0$

Walls of tubes, interfaces of fluid & solid which are assumed to be of no-slip condition & having conjugate heat transfer in-between them have following boundary conditions-

$u = v = w = 0$ & $-\lambda_f \cdot \frac{\partial T_F}{\partial y} = -\lambda_s \cdot \frac{\partial T_s}{\partial y}$

Baffles, interfaces of fluid & solid which are assumed to be of no-slip condition & having conjugate heat transfer in-between them have following boundary conditions-

$u = v = w = 0$ & $-\lambda_f \cdot \frac{\partial T_F}{\partial x} = -\lambda_s \cdot \frac{\partial T_s}{\partial x}$

where, f=fluid (water) and s=solid (Aluminium walls)

Mesh & Computational Model

A 3D model of a heat exchanger and grids was created using ANSYS Workbench. A high-quality tetrahedral and hexahedral mesh was utilized in the modeling, as seen in Figure 3. The meshes consist of 936,375 elements for the heat exchanger without baffles, and 964,776 elements with baffles. The governing equations were solved using the FLUENT code, which is based on the finite volume approach and the SIMPLE algorithm. The energy, momentum, kinetic energy of turbulence, and dissipation rate were approximated using the first-order upwind scheme. However, the pressure term was handled using the more accurate second-order upwind method.

The convergence criteria for all variables were set at 10^{-3}. The relaxation factors for the energy equation, momentum equations, kinetic energy of turbulence, pressure correction equation, and turbulence dissipation rate were assigned the values of 1, 0.5, 0.8, 0.3, and 0.8, respectively.

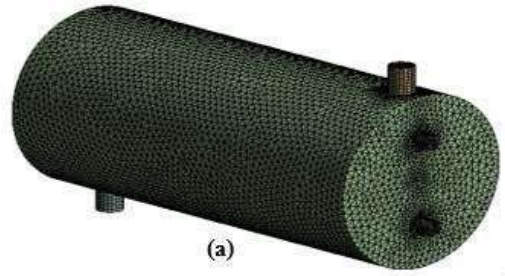

(a)

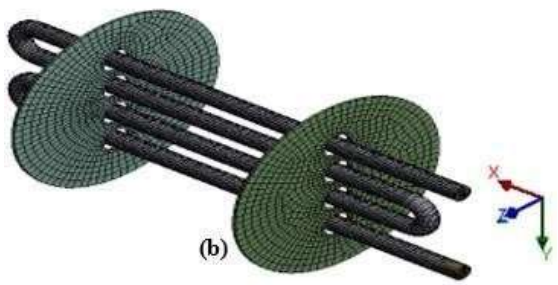

(b)

Figure 3. Meshing of the physical model: (a) heat exchanger without baffles, (b) partial meshes of baffles and tube

Methodology for Exergy

The exergy of a system is defined as the highest amount of useful work that may be extracted from the system when it reaches equilibrium with its surroundings. The shaft work of the HX is negligible, hence the exergy is obtained from the same flowing fluids and is defined by the exergy balance.

The exergy loss for a stable control volume may be computed using the relationship provided in reference [7].

$$Ex_{loss} = T_O[\dot{m}_c C_{pc} ln(T_{c,out}/T_{c,in}) + \dot{m}_h C_{ph} ln(T_{h,out}/T_{h,in})]$$

The exergy efficiency is calculated by dividing the change in availability of the cold stream by the change in availability of the hot stream.

$$\eta_{\Pi} = \frac{\dot{m}_w(\Psi_{w,o} - \Psi_{w,i})}{\dot{m}_h(\Psi_{h,i} - \Psi_{h,o})}$$

Where,

$$\dot{m}_c(\Psi_{c,o} - \Psi_{c,i}) = \dot{m}_c[(h_{c,o} - h_{c,i}) - T_o(s_{c,o} - s_{c,i})]$$

$$\dot{m}_h(\Psi_{h,i} - \Psi_{h,o}) = \dot{m}_h[(h_{h,i} - h_{h,o}) - T_o(s_{h,i} - s_{h,o})]$$

In which, $\dot{m}c$ and $\dot{m}h$ refer to mass flow rate of cold and hot respectively; $(\psi_{c,o} - \psi_{c,i})$ is the availability change between the outlet cold and inlet cold; $(\psi_{h,i} - \psi_{h,o})$ is the availability change between inlet hot and outlet hot; h and s stand for enthalpy and entropy respectively and To is environment temperature.

Results & Discussion

Grid independent study

To obtain accurate results with good grid, three different grid sizes are tested and shown in Table 2. The illustrates the results of grid independent for the outlet temperature of the shell side with Reynolds number of tube side for heat exchanger without and with baffles as seen in Figure 4. It can be noted from figure that, there is no significant change on the results when the grid sizes increase and only the operation time increases. Therefore, a grid containing 936375 cells and 964776 cells are employed in this study for heat exchanger without and with baffles respectively.

Characterization of thermal and hydraulic behaviors

Figure 5 shows 2D temperature distribution contours at a longitudinal central plane of a complete heat exchanger unit (shell and double tube) at (x-y) plane. It is noticed that, the temperature of hot water on the side of the shell decreased along the heat exchanger, while the cold-water temperature from the side of the pipe gradually increases for both heat exchangers. In Figure 5 (b), it can be noted that the temperature difference between the inlets and outlets of the heat exchanger is high compared to Figure 5 (a). This is due the presence the baffles that generate the high turbulence swirling leading to increase the heat transfer between two liquids. This means that the hot water stays longer in the heat exchanger, increasing the time available to heat transfer to the cold water. For these cases, the tube outlet temperature was increased by about 308 K for without baffles, 312 K for with baffles, while shell outlet temperature was decreased by about 347 K for without baffles, 340 K for with baffles.

The 3D streamlines plots of hot water flow along the heat exchanger are shown in Figure 6 at Reshell=4000. Figure 6 (a) appears that the most of hot water flows uniformly and longitudinally towards the shell outlet. In Figure 6 (b), the acceleration and expansion of the hot fluid flow across baffles can be observed along the HX. The results explain that the presence of baffles caused the flow direction varies, which produces multi-directional stream, then lead to enhancement in the turbulence. This is due to a decrease in the area of flow of the vents on the baffles and thus leads to a sharp increase in velocity. So, the highest velocity of 0.06 m/s is observed near the circular vents compared to surface far away from the vents. Since the baffle block, the hot water flow in front of the baffles from the center to the shell edge and then the hot water flows across the baffles back to the center form the edge, leading to the production of a secondary flow that promotes the heat transfer of the shell side. Figure 7 shows the effect of both the baffles and tube Reynolds number on heat exchanger effectiveness which is defined as:

$$\varepsilon = \frac{Q_{actual}}{Q_{max}} = \frac{\dot{m}_c c_p(T_{hi} - T_{ho})}{(\dot{m} c_p)_{min}(T_{hi} - T_{wi})}$$

Table 2. Grid independent study

Grid	Grid size of heat exchanger withoutbaffles	Grid size of heat exchanger with baffles
Grid I	936375	964776
Grid II	940772	969171
Grid III	943939	975950

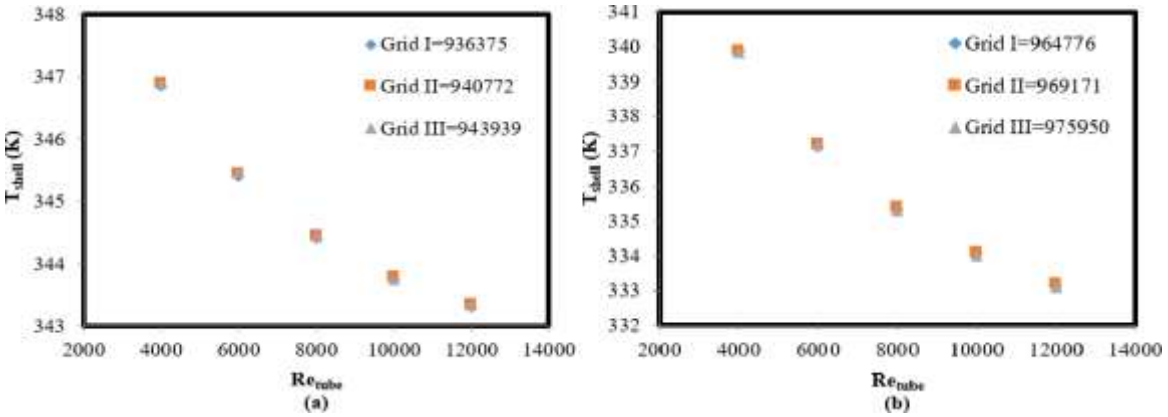

Figure 4. Grid independence test results for numerical solution of heat exchanger at Reshell=4000: (a) without baffles, (b) with baffles

It is evident that the HX with baffles exhibits greater effectiveness values compared to the one without baffles. This is attributed to the circular vents present on the baffles, which induce turbulence and random movement in the flow field. As a result, heat transfer between fluids is enhanced. The heat exchanger efficacy is around 34 - 45% lower when baffles are present compared to when they are absent. Simultaneously, it is noted that the efficacy of the system improved as the Reynolds number of the cold water grew, owing to the higher velocity. These results are consistent with the findings of reference [8].

Figure 8 illustrates the relationship between the pressure drop on the shell side and the shell Reynolds number. The findings indicate that the HX equipped with baffles exhibits a substantial increase in pressure drop. This suggests that the baffles serve as both a guiding mechanism and an obstruction to the flow, resulting in an elevation in the pressure drop. In a heat exchanger without baffles, the fluid flow typically follows a path from the entry to the exit. Consequently, the only factors contributing to pressure drop are the fluid's movement throughout the pipe and the friction it experiences along the shell's wall. Consequently, the installation of baffles will impede the movement of fluids in the intended direction, resulting in an elevation of pressure drop. Furthermore, the pressure drops in both heat exchangers increases gradually as the shell Reynolds number increases, which is a result of the increased velocity.

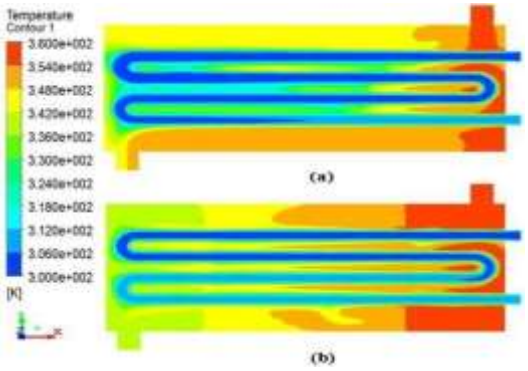

Figure 5. Contours of temperature distribution at a longitudinal central plane for heat exchanger at Re=4000: (a) without baffles, (b) with baffles

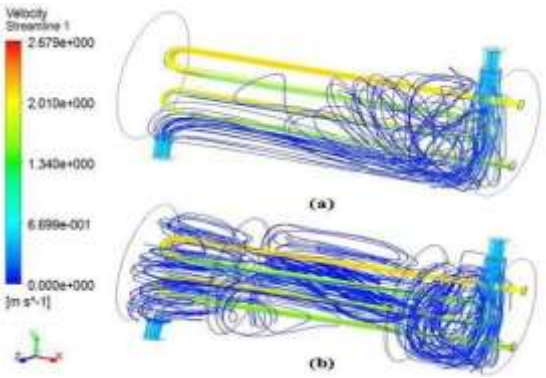

Figure 6. Streamlines plots of hot water flow along heat exchanger at Re=4000: (a) without baffles, (b) with baffles

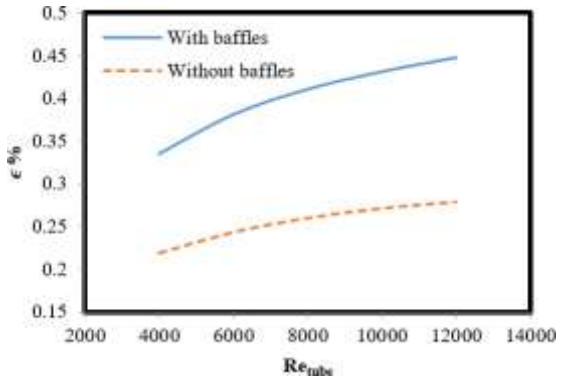

Figure 7. Effect of both the baffles and tube Reynolds number on heat exchanger effectiveness

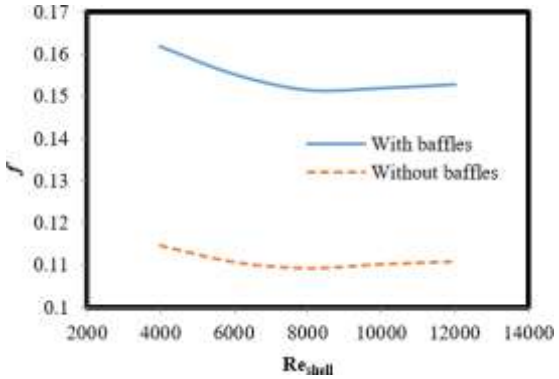

Figure 8. Variation of pressure drop of shell side vs. shell Reynolds number

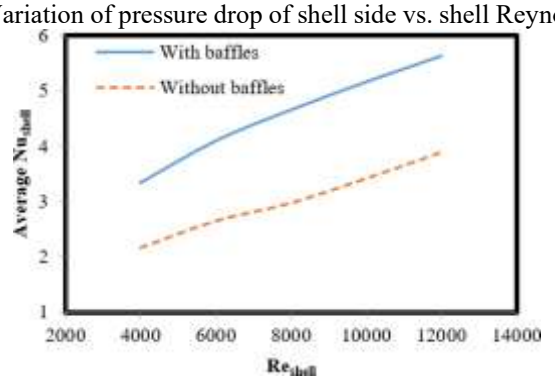

Figure 9. Variation of shell friction coefficient value on various Reynolds number of the shell

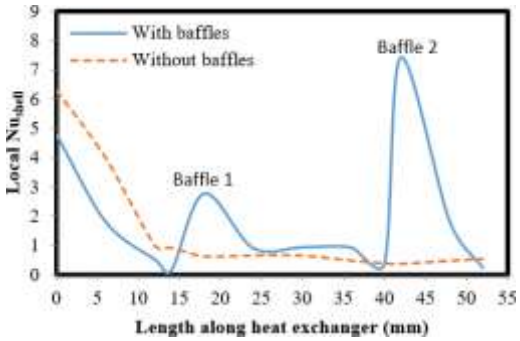

Figure 10. The effect of both the baffles and tube Reynolds number on average Nu of tube side

$$f = \frac{2D_h \Delta P}{\rho L u^2}$$

The graphic demonstrates that the friction coefficient of HX is lower when there are no baffles compared to when there are baffles present. The results indicated that the coefficient of friction reduced when the shell Reynolds number increased for both heat exchangers, as a result of the increased velocity. This was consistent with fluid dynamics, where the friction coefficient exhibited a straight inverse relationship with velocity.

Figure 10 illustrates the impact of both baffles and tube Reynolds number on the average Nusselt number of the tube side. The average Nu value is determined by numerically integrating the local Nu values along the heat exchanger (HX) using the trapezoidal method.

$$\bar{\bar{\bar{N}}}_u = \frac{1}{L}\int_0^L Nu\, dx$$

The chart clearly demonstrates that baffles have a significant impact on the average Nusselt number for heat exchangers. This suggests that the Nusselt number is increased due to vigorous fluid mixing caused by the baffles. The Nusselt number reaches a maximum value of roughly 5.7 in this particular example. Furthermore, the Nusselt number exhibits a positive correlation with the Reynolds number of the cold water, since this leads to an increase in the heat transfer coefficient of the heat exchanger. These results corroborate the findings of Yang and Liu [14].

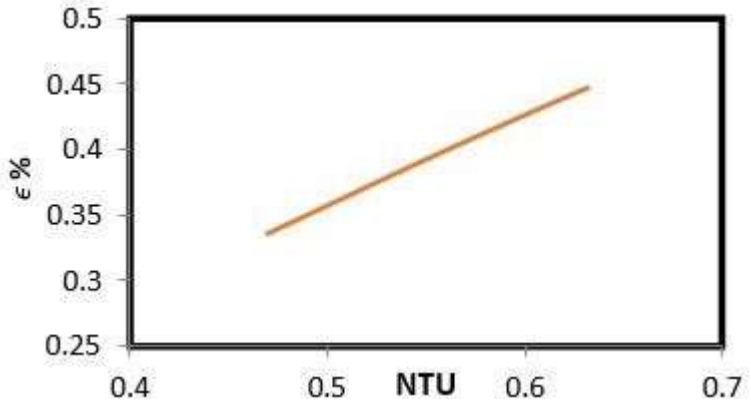

Figure 11. Local Nusselt number distribution along flow direction at various shell Reynolds number

The distribution of local Nusselt number along flow direction of shell side for various Reynolds numbers is shown in Figure 11, which is expressed as:

$$Nu_{local} = \bar{h}_{(CFD)} D_h / K_f$$

The graphic clearly illustrates that heat exchangers with baffles exhibit greater Nusselt number values. The greatest value of 7.5 is recorded near the baffle positioned at the heat exchanger outlet. In contrast, heat exchangers without baffles show a reduction in Nusselt number towards the exit, reaching a constant value.

Figure 12 depicts the relationship between NTU (Number of Transfer Units) and efficacy for a Heat Exchanger (HX) equipped with baffles. The values of NTU are calculated by:

$$NTU = \frac{UAs}{(\dot{m} C_p)_{min}}$$

Where

$$\frac{1}{U} = \frac{1}{h_i} + \frac{\delta_t}{k_t} + \frac{1}{h_o}$$

As can be shown, by increasing in the effectiveness, the NTU is also increased. These results are an agreement with previous results.

It is show that the exergy loss increases as increasing Reynolds number of cold water for both heat exchangers. The exergy loss of the HX with baffles is larger than that without baffles. The highest value of exergy loss is about of 42 W for this case. This reason is due to presence of circular holes on the baffles are gives high swirling, which increase of heat transfer rate. Moreover, the heat transfer rate increases with increased temperature difference between the inlets and outlets fluids. This parameter plays an important role for exergy loss. These results are an agreement to Etghani and Baboli [7].

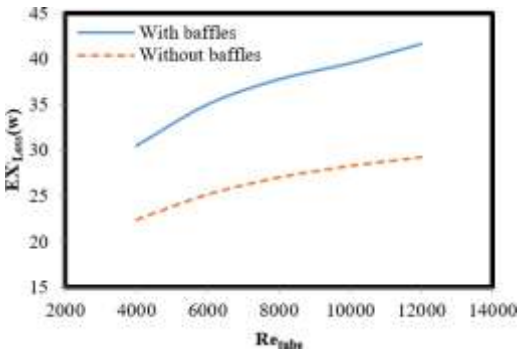

Figure 12. Variation of exergy loss vs. different tube Reynolds number

Figure 13. Exergy efficiency vs. tube Reynolds numbers

Figure 14 shows the exergy efficiency versus tube Reynolds numbers. The value of exergy efficiency is computed by Eq. (10). It is appeared that the efficiency of each HX is decreased with increasing tube Reynolds numbers due to increased temperature difference between inlet and outlet fluids leading to reduced entropy. This result is an agreement well with Bashtani and Esfahani [17].

Conclusions

We are now doing research on the thermal behavior and exergy analysis of the shell and double tube heat exchanger, which plays a crucial role in many energy conversion processes. The ANSYS (Fluent) program was used to generate a three-dimensional model of the shell and double tube heat exchanger, both with and without

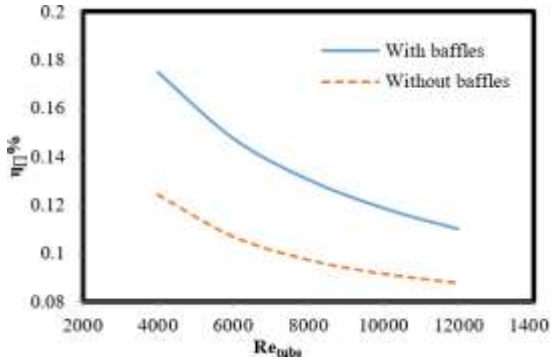

circular vent baffles. The primary findings may be succinctly described as follows:

- The presence of baffles in the HX significantly enhances its efficacy by approximately 17% at high Reynolds numbers compared to when baffles are not present.
- The findings demonstrated that the heat exchanger (HX) equipped with baffles attained the maximum Nusselt number and pressure drop in relation to the Reynolds number.
- The inclusion of baffles in the HX results in higher levels of loss and exergy efficiency compared to when baffles are not present.

Ultimately, it was determined that the HX with baffles exhibits superior thermal and hydraulic performance compared to the one without baffles. This is due to the design's ability to augment the surface area and prolong the fluid's residence time, resulting in greater heat transfer. Furthermore, the ANSYS Fluent software was essential in forecasting the thermal and hydraulic characteristics of the twin tube heat exchanger.

References

[1] Adrain B (2002) Fundamentals of exergy analysis, entropy generation minimization, and the generation of flow architecture. Int J Energy Res 26:0–43
[2] Afsar, N., Inam, M.I. (2018). CFD analysis of shell and tube heat exchanger with different baffle orientation and baffle cut. AIP Conference Proceedings, 1980(1): 050006. https://doi.org/10.1063/1.5044342
[3] Ahmadi, G.; Toghraie, D.; Akbari, O.A. Solar parallel feed water heating repowering of a steam power plant: A case study in Iran. Renew. Sustain. Energy Rev. 2017, 77, 474–485.
[4] Ahmadi, G.R.; Toghraie, D. Energy and exergy analysis of Montazeri steam power plant in Iran. Renew. Sustain. Energy Rev. 2016, 56, 454–463.
[5] Akpinar EK (2006) Evaluation of heat transfer and exergy loss in a concentric double pipe exchanger equipped with helical wires. Energy Convers Manag 47:3473–3486
[6] Ali S (2001) Pressure drop correlations for flow through regular helical coil tubes. Fluid Dynamics Res 28(4):295
[7] Alimoradi A (2017) Investigation of exergy efficiency in shell and helically coiled tube heat exchangers. Case Stud Thermal Eng 10:1–8
[8] Alimoradi A, Olfati M, Maghareh M (2017) Numerical investigation of heat transfer intensification in shell and helically coiled finned tube heat exchangers and design optimization. Chem Eng Process Intensif 121:125–143
[9] Alimoradi A, Veysi F (2016) Prediction of heat transfer coefficients of shell and coiled tube heat exchangers using numerical method and experimental validation. Int J Therm Sci 107:196–208
[10] Amori KE (2014) Thermal and hydraulic characteristics of a novel helical coiled tube used as a heat exchanger. Arab J Sci Eng 39: 4179–4186
[11] Andrzejczyk R, Muszynski T (2017) Thermodynamic and geometrical characteristics of mixed convection heat transfer in the shell and coil tube heat exchanger with baffles. Appl Thermal Eng 121: 115–125
[12] Baqir AS, Mahood HB, Kareem AR (2019) Optimization and evaluation of NTU and effectiveness of a helical coil tube heat exchanger with air injection. Thermal Sci Eng Progress 14:100420

[13] Bashtani, I., Esfahani, J.A. (2019). ε - NTU analysis of turbulent flow in a corrugated double pipe heat exchanger: A numerical investigation. Applied Thermal Engineering, 159: 113886. https://doi.org/10.1016/j.applthermaleng.2019.113886
[14] Belitor, J.N.P.; Pabilona, L.; Villanueva, E. A Performance Evaluation and Optimization of a 135-Mw Circulating Fluidized Bed (CFB) Coal Based Thermal Power Plant Turbine Cycle Using Exergy Analysis. Innov. Ener. Res. 2018, 7, 1463–2576.
[15] Bhuiyan AA, Amin MR, Islam AKMS (2013) Three-dimensional performance analysis of plain fin tube heat exchangers in transitional regime. Appl Therm Eng 50:445–454
[16] Brassard, P.; Palacios, J.H.; Godbout, S.; Bussières, D.; Lagacé, R.; Larouche, J.P.; Pelletier, F. Comparison of the gaseous and particulate matter emissions from the combustion of agricultural and forest biomasses. Bioresour. Technol. 2014, 155, 300–306.
[17] Celen, A. Energy and exergy analysis of a shell and tube heat exchangers having smooth and corrugated inner tubes. Süleyman Demirel Üniversitesi Fen Bilim. Enstitüsü Derg. 2022, 26, 171–181.
[18] Dančová P, Hussain A, Fsadni AM, Veselý M (2016) CFD analysis of the two-phase bubbly flow characteristics in helically coiled rectangular and circular tube heat exchangers. EPJ Web of Conferences 114:02044
[19] Dias, R.A.; Balestieri, J.A.P. Energetic and exergetic analysis in a firewood boiler. Rev. De Cienc. Tecnol. 2004, 12, 15–24.
[20] Dincer, I.; Cengel, Y.A. Energy, entropy and exergy concepts and their roles in thermal engineering. Entropy 2001, 3, 116–149.
[21] Dizaji, H.S.; Khalilarya, S.; Jafarmadar, S.; Hashemian, M.; Khezri, M. A comprehensive second law analysis for tube-in-tube helically coiled heat exchangers. Exp. Therm. Fluid Sci. 2016, 76, 118–125.
[22] Dooner, M.; Wang, J. Compressed-air energy storage. In Future Energy; Elsevier: Amsterdam, The Netherlands, 2020; pp. 279–312.
[23] dos Santos Filho, S.J., de Souza, J.S., de Lima, A.G.B. (2017). Numerical simulation of the shell-and-tube heat exchanger: Influence of the lower flows and the baffles on a fluid Dynamics. Advances in Chemical Engineering and Science, 7(4): 78727. https://doi.org/10.4236/aces.2017.74026
[24] Emani MS, Ranjan H, Bharti AK, Meyer JP, Saha SK (2019) Laminar flow heat transfer enhancement in square and rectangular channels having: (1) a wire-coil, axial and spiral corrugation combined with helical screw-tape with and without oblique teeth and a (2) spiral corrugation combined with twisted tapes with oblique teeth. Int J Heat Mass Transf 144:118707
[25] Esen, H.; Inalli, M.; Esen, M.; Pihtili, K. Energy and exergy analysis of a ground-coupled heat pump system with two horizontal ground heat exchangers. Build. Environ. 2007, 42, 3606–3615.
[26] Esfahani, M.R.; Languri, E.M. Exergy analysis of a shell-and-tube heat exchanger using graphene oxide nanofluids. Exp. Therm. Fluid Sci. 2017, 83, 100–106.
[27] Etghani, M.M., Baboli, S.A.H. (2017). Numerical investigation and optimization of heat transfer and exergy loss in shell and helical tube heat exchange. Applied Thermal Engineering, 121: 294-301. http://dx.doi.org/10.1016/j.applthermaleng.2017.04.074
[28] Fahad, S., Alshara, A.K., Saeed, M. (2017). Numerical investigation of heat transfer and flow characteristics in shell and U-tube heat exchanger with baffles. Journal of University of Duhok, 20: 404-415. https://doi.org/10.26682/sjuod.2017.20.1.37
[29] Gulhane, S.J.; Thakur, A.K. Exergy analysis of boiler in cogeneration thermal power plant. Am. J. Eng. Res. 2013, 2, 385–392.
http://www.iaeme.com/IJMET/index.asp.
[30] Irshad, M., Kaushar, M., Rajmohan, G. (2017). Design and CFD analysis of shell and tube heat exchanger. International Journal of Engineering Science and Computing, 7(4): 6453-6457.
[31] James, C.; Kim, T.Y.; Jane, R. A Review of Exergy Based Optimization and Control. Processes 2020, 8, 364.
[32] Kallannavar, S.; Mashyal, S.; Rajangale, M. Effect of tube layout on the performance of shell and tube heat exchangers. Mater. Today: Proc. 2020, 27, 263–267.
[33] Kirinčić, M., Trp, A., Lenić, K. (2017). Numerical investigation and experimental validation of heat transfer in a small size shell and tube heat exchanger. Engineering Review, 37(2): 122-133.
[34] Kline SJ, FA MC (1953) Describing uncertainties in single-sample experiments. Mech Eng 78:3–8
[35] Kulkarni, H.R.; Revankar, P.P.; Hadagal, S. Energy and Exergy Analysis of Coal Fired Power Plant. Int. J. Innov. Res. Technol. Sci. 2014, 11, 53–57.
[36] Kumar R, Chandra P (2019) Thermal analysis, pressure drop and exergy loss of energy efficient shell, and triple meshed helical coil tube heat exchanger, energy sources, part a: recovery, utilization, and environmental effects, 42(8):1026–1039. https://doi.org/10. 1080/15567036.2019.1602213
[37] Mandal MM, Serra C, Hoarau Y, Nigam KDP (2010) Numerical modeling of polystyrene synthesis in coiled flow inverter. Microfluid Nanofluid 10:415–423
[38] Mehdizadeh-Fard, M.; Pourfayaz, F. Advanced exergy analysis of heat exchanger network in a complex natural gas refinery. J. Clean. Prod. 2019, 206, 670–687.
[39] Mert, S.O.; Reis, A. Experimental performance investigation of a shell and tube heat exchanger by exergy-based sensitivity analysis. Heat Mass Transf. 2016, 52, 1117–1123.
[40] Mule, B.A., Hatkar, D.N., Bembde, M.S. (2017). Analysis of double pipe heat exchanger with helical fins.

International Research Journal of Engineering and Technology, 4(8): 2395-0072.
[41] Naphon P (2011) Study on the exergy loss of the horizontal concentric micro-fin tube heat exchanger. Int Commun Heat Mass Transfer 38:229–235
[42] Nilsson, D. Energy, exergy and energy analysis of using straw as fuel in district heating plants. Biomass Bioenergy 1997, 13, 63–73.
[43] Pamuk, M.T. (2019). Numerical investigation of the effects of the baffles added in a concentric pipe heat exchanger. International Journal of Heat and Technology, 37(2): 583-588. https://doi.org/10.18280/ijht.370228
[44] Pandey SD, Nema VK (2011) An experimental investigation of exergy loss reduction in corrugated plate heat exchanger. Energy 36:2997–3001
[45] Pawar SS, Sunnapwar VK (2013) Studies on convective heat transfer through helical coils. Heat Mass Transf 49:1741–1754
[46] Qian, X.; Lee, S.; Chandrasekaran, R.; Yang, Y.; Caballes, M.; Alamu, O.; Chen, G. Electricity evaluation and emission characteristics of poultry litter co-combustion process. Appl. Sci. 2019, 9, 4116.
[47] Qian, X.; Lee, S.W.; Yang, Y. Heat transfer coefficient estimation and performance evaluation of shell and tube heat exchanger using flue gas. Processes 2021, 9, 939.
[48] Rahimi M, Ardahaie SS, Hosseini MJ, Gorzin M (2020) Energy and exergy analysis of an experimentally examined latent heat thermal energy storage system. Renew Energy 147:1845–1860
[49] Rant, Z. Exergy, a new word for technical available work. Forsch. Ing. Wis. 1956, 22, 36–37.
[50] Riyandwita BW, Awwaluddin M, Hastuty S (2019) Performance evaluation of helical coil heat exchanger with annulus shell side using computational fluid dynamics. AIP Conference Proc 2193:020039
[51] Sadighi Dizaji H, Jafarmadar S, Hashemian M (2015) The effect of flow, thermodynamic and geometrical characteristics on exergy loss in shell and coiled tube heat exchangers. Energy 91:678–684
[52] Sadighi Dizaji H, Khalilarya S, Jafarmadar S, Hashemian M, Khezri M (2016) A comprehensive second law analysis for tube-in-tube helically coiled heat exchangers. Experiment Thermal Fluid Sci 76:118–125
[53] Sadikin, A., Khian, N.Y., Hwey, Y.P., Al-Mahdi, H.Y., Taib, I., Sadikin, A.N., Salleh, S.M., Ayop, S.S. (2018). Effect of number of baffles on flow and pressure drop in a shell side of a shell and tube heat exchangers. Journal of Advanced Research in Fluid Mechanics and Thermal Sciences, 48(2): 156-164.
[54] Santhisree, N., Prashanthkumar, M., Priyanka, G. (2017). Thermal analysis of shell and tube heat exchanger. International Journal of Mechanical Engineering and Technology, 8(5): 596-606.
[55] Sharqawy MH, Saad SMI, Ahmed KK (2019) Effect of flow configuration on the performance of spiral-wound heat exchanger. Appl Therm Eng 161:114157
[56] Sheeba A, Akhil R, Prakash MJ (2020) Heat transfer and flow characteristics of a conical coil heat exchanger. Int J Refrig 110: 268–276
[57] Shriwas, D., Saini, J., Sahu, P.K. (2018). Numerical simulation and CFD analysis of double tube heat exchanger with different tube geometries on same cross section area. International Journal for Scientific Research, 6(5): 2321-0613.
[58] Singh, D.S., Pal, N.D. (2016). Designing and performance evaluation of a shell and tube heat exchanger using Ansys. International Journal of Scientific Engineering and Applied Science, 2(3): 2395- 3470.
[59] Teja, G.V., Narasimha Rao, K.V. (2017). Numerical investigation on heat transfer and fluid flow of shell-side for shell and tube heat exchanger with hexagonal vent baffle by using CFD. International Journal of Mechanical Engineering and Technology, 8(5): 995-1009.
[60] Terzi, R. Application of exergy analysis to energy systems. In Application of Exergy; In Tech Open: London, UK, 2018; p. 109.
[61] Vocale P, Bozzoli F, Rainieri S, Pagliarini G (2019) Influence of thermal boundary conditions on local convective heat transfer in coiled tubes. Int J Therm Sci 145:106039
[62] Whitely, N.; Ozao, R.; Artiaga, R.; Cao, Y.; Pan, W.P. Multi-utilization of chicken litter as biomass source. Part I. Combustion. Energy Fuels 2006, 20, 2660–2665.
[63] Wu S-Y, Chen S-J, Li Y-R, Li L-J (2008) Numerical investigation of turbulent flow, heat transfer and entropy generation in a helical coiled tube with larger curvature ratio. Heat Mass Transf 45:569–578
[64] Yang, J., Liu, W. (2015). Numerical investigation on a novel shell-and-tube heat exchanger with plate baffles and experimental validation. Energy Conversion and Management, 101: 689-696. http://dx.doi.org/10.1016/j.enconman.2015.05.066
[65] You, Y., Chen, Y., Xie, M., Luo, X., Jiao, L., Huan, S. (2015). Numerical simulation and performance improvement for a small size shell-and tube heat exchanger with trefoil-hole baffles. Applied Thermal Engineering, 89: 220-228. https://doi.org/10.1016/j.applthermaleng.2015.06.012
[66] Zhang, L.; Xia, Y.; Jiang, B.; Xiao, X.; Yang, X. Pilot experimental study on shell and tube heat exchangers with small-angles helical baffles. Chem. Eng. Process. Process Intensif. 2013, 69, 112–118.
[67] Zhou, G., Xiao, J., Zhu, L., Wang, J., Tu, S. (2015). A numerical study on the shell-side turbulent heat transfer enhancement of shell and tube heat exchanger with trefoil hole baffles. Energy Procedia, 75: 3174-3179. https://doi.org/10.1016/j.egypro.2015.07.656